Gas-Phase Electronic Spectra of Two Substituted Benzene Cations: Phenylacetylene + and 4-Fluorostyrene +

ARTICLE *in* THE JOURNAL OF PHYSICAL CHEMISTRY A · DECEMBER 2007

Impact Factor: 2.69 · DOI: 10.1021/jp073381c · Source: PubMed

4 AUTHORS, INCLUDING:

Thomas Pino
Université Paris-Sud 11
83 PUBLICATIONS **856** CITATIONS
SEE PROFILE

Stéphane Douin
Université Paris-Sud 11
41 PUBLICATIONS **390** CITATIONS
SEE PROFILE

Gas-Phase Electronic Spectra of Two Substituted Benzene Cations: Phenylacetylene$^+$ and 4-Fluorostyrene$^+$

T. Pino,* S. Douin, N. Boudin, and Ph. Bréchignac

Laboratoire de Photophysique Moléculaire,† CNRS, bâtiment 210 Université Paris-Sud, F-91405 Orsay Cedex, France

Received: May 3, 2007; In Final Form: September 21, 2007

The visible spectra of phenylacetylene$^+$ and 4-fluorostyrene$^+$ have been measured by laser photodissociation spectroscopy. The observed vibronic systems were assigned to the $\tilde{B}^2A'' \leftarrow \tilde{X}^2A''$ and $\tilde{C}^2B_1 \leftarrow \tilde{X}^2B_1$ electronic transition in the 4-fluorostyrene$^+$ and phenylacetylene$^+$ cations, respectively. Two methods were employed and compared: a resonant multiphoton dissociation scheme of the bare cations and a resonant photodissociation technique applied to the chromophore$^+$−argon$_{n=1,2}$ ionic complexes. The latter approach allowed the intrinsic profile to be resolved, revealing different intramolecular dynamical behavior. Their electronic relaxation has been rationalized in terms of an apparent energy gap law for the benzene derivative cations.

I. Introduction

During the last two decades, the electronic spectroscopy of aromatic cations has been explored largely due to the development of derivatives of the resonantly enhanced multiphoton ionization (REMPI) technique as tools to prepare the cations in a well defined state. Various methods have been developed, including laser induced fluorescence,[1] resonant enhanced multiphoton photodissociation spectroscopy (REMPDS),[2,3] photoinduced Rydberg ionization (PIRI),[4] and laser photoelectron spectroscopy (PES).[5] Recently, cold ion trapping with REMPDS has proven to be a powerful tool for the investigation of the electronic spectroscopy of cations in the gas phase.[6] Photodissociation spectroscopy of weakly bound ionic complexes has also been shown to be a powerful tool where the weakly bound atom acts as a probe of the chromophore[7,8] even in electronically excited states.[9−11] The electronic spectra of the benzene cation and some of its derivatives, such as the halobenzenes, have thus been obtained.[2,4,12−19] In the past their electronic structure has been mainly investigated by PES,[20] and fluorescence spectra have been measured where possible.[21−23]

The present study of aromatic cations is motivated by fundamental aspects, although the two compounds on which we focus, 4-fluorostyrene and phenylacetylene, are of importance in polymerization reactions. In the investigation of various phenomena such as electronic structure, substitution effects, and radiationless transitions,[24,25] large aromatic molecules have often served as models as they form a coherent molecular series. Relevant spectroscopic studies revealed strong vibronic coupling in the monosubstituted benzene cations where vibronically induced transitions could be observed in the visible to near UV regions. For example, in the case of phenol$^+$, strong geometry changes upon electronic excitation were found to involve the OH substituent,[4] but for aniline$^+$ a strong ring geometry change was found.[5,26] For the polyfluorobenzene$^+$ cations, the occurrence of the well-documented energy gap law for nonradiative transitions was demonstrated for the $\tilde{B}$ state.[27]

In the present paper, we report the visible gas-phase spectra of two benzene derivatives, phenylacetylene$^+$ (PA$^+$) and 4-fluorostyrene$^+$ (4FSTY$^+$), making further progress in the investigation of substituted benzene cations.

Neutral PA and 4FSTY molecules and their van der Waals complexes chromophore−argon$_n$ have been studied in detail,[28−34] and the electronic spectrum of PA$^+$ measured by the PIRI approach was recently published.[35] To monitor the visible spectra of the cations, two spectroscopic techniques were be employed for both compounds, namely the rare gas tagging approach and the REMPDS technique. This allowed the different capacities of the methods to be explored. The combination of these experiments permitted investigation of the intramolecular dynamics as revealed by frequency resolved profiles.

II. Experimental Details

The molecular beam-time-of-flight (TOF) mass spectrometer apparatus has already been described.[36,37] Phenylacetylene or 4-fluorostyrene (both Aldrich) vapor were produced in the sample chamber at room temperature and seeded in a mixture of Ar diluted in He with a backing pressure ∼5 bar. Both chemicals were used without any further purification. The gas was expanded through the 0.9 mm orifice of a pulse solenoid valve, the temporal pulse length being 230 μs.

The cations were produced by resonant two-photon ionization in the extraction zone of the TOF. Different schemes have been used. First, a resonant one-color two-photon ionization (R2PI) scheme was implemented, resulting in ∼700 cm^{-1} of excess energy above the ionization threshold in the case of PA$^+$ and about 400 cm^{-1} in the case of 4FSTY$^+$. When available, the photoelectron spectra revealed that the cations prepared by this scheme are mostly in their vibrationless level,[28,38,39] although a non-negligible contribution of a mode at about 450 cm^{-1} is expected for PA$^+$. Additional experiments were performed, ionizing PA through a vibronic band belonging to the $S_1 \leftarrow S_0$ electronic transition, allowing the preparation of the cation initially in its 35_1 level, following Mulliken notation,[40] with about 450 cm^{-1} of vibrational energy. The details are discussed in the last section. The second ionization scheme was a resonant two-color two-photon scheme (R2C2PI) to diminish the excess

† Laboratoire associé à l'Université Paris-Sud, membre de la Fédération de recherche Lumière Matière.

10.1021/jp073381c CCC: $37.00
Published on Web 12/04/2007

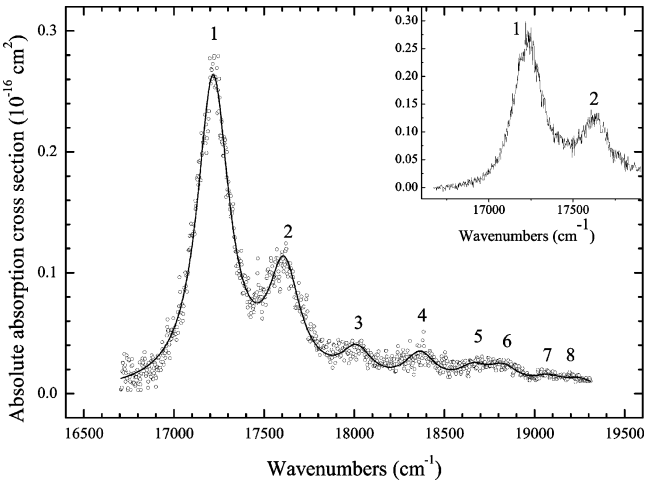

Figure 1. Photodissociation spectrum of the $C_8H_7F-Ar_2$ ionic complex prepared by a resonant one-color two-photon scheme. The inset is the region of the origin band observed in the photodissociation spectra of $C_8H_7F^+-Ar$ prepared by a resonant one-color two-photon scheme. The vertical scales are the absolute absorption cross section (given in 10^{-16} cm^2) for both spectra. The labels of the bands are those used in Table 1.

energy in the cation to a few cm^{-1}, thus enabling one to check for the appearance of hot and/or sequence bands arising from the excitation of intramolecular or intermolecular motions following cation preparation. This scheme was only applied to PA$^+$. The photodissociation spectra were obtained by scanning a third pulsed laser (unfocussed) fired into the ion cloud a few hundred nanoseconds after ionization. It should be noted that because the electronic shift due to argon solvation depends on the binding site on the aromatic molecule,[41] the absorption spectrum of the cationic chromophore can be deduced by monitoring the photodissociation spectra of the chromophore$^+-$Ar (1/0) and chromophore$^+-$Ar$_2$ (1/1) complexes,[10,11] and extrapolating to the bare cation. The notations (1/0) and (1/1) denote the isomers with the argon atoms occupying the "ring" binding sites with one argon atom per site. Where photodissociating the bare cations, several ionic fragmentation channels were monitored. Mass spectra were also measured at fixed photodissociation wavelength while the energy per pulse was varied. This technique enabled the absolute photodissociation cross section to be deduced as thoroughly explained earlier.[10]

For PA, a frequency-doubled output of a dye laser pumped by an excimer laser ($h\nu \approx 35\,800$ cm^{-1} [28]) was used to perform either the R2PI or the excitation step $S_1 \leftarrow S_0$ in the R2C2PI experiment. The frequency-doubled output of a dye laser pumped by a frequency-doubled Nd:YAG laser was used for the ionization step. For 4FSTY, the latter laser ($h\nu \approx 34\,300$ cm^{-1} [29]) was used for the R2PI cation preparation. In both cases, a commercial optical parametric oscillator (0.2 cm^{-1} bandwidth) was used to photodissociate the cations. All of these lasers were synchronized and fired in the center of the extraction zone of the TOF apparatus. The ion current collected by a microchannel plate detector was fed into a digital oscilloscope after preamplification with experiments being driven by Labview programs. The fragment(s) and parent currents were monitored as a function of the photodissociation laser wavelength and intensity. In the photodissociation experiments of the ionic complexes, the chromophore$^+$ fragment was monitored.

III. Results and Analysis

A. 4-Fluorostyrene Cation. The photodissociation spectrum of 4FSTY$^+-$argon$_2$ (1/1) is shown in Figure 1, with a zoom of the lowest part of the band system for 4FSTY$^+-$argon (1/0). The cations were prepared by the R2PI scheme. The spectra are corrected for the photodissociation laser intensity variations and scaled to the absolute absorption cross section according to the method described earlier in ref 10. Two types of scan were recorded: survey scans, as shown in Figure 1 with large wavelength steps, and high-resolution scans with the small wavelength steps to exploit the laser resolution (about 0.2 cm^{-1}). The latter did not reveal any substructures, even after decreasing the photodissociation laser fluence. Indeed, special care was taken to avoid power saturation effects to ensure that no additional sources of broadening were introduced. Thus, intrinsic intensity ratios were measured. Owing to the broadness of the observed features, a Lorentzian fit of the vibronic bands with a unique bandwidth was used to determine the band frequencies and thus guide the assignment. However, it should be noted that significant spectral congestion is present: the full width at half-maximum (fwhm) is found to be 215 ± 20 cm^{-1} for 4FSTY$^+-$argon$_2$ (1/1) and 170 ± 15 cm^{-1} for 4FSTY$^+-$argon (1/0).

TABLE 1: Band Center Positions (Absolute ν and Relative $\delta\nu$) and Absolute Absorption Cross Section (σ_{abs}) Obtained from the Photodissociation Spectrum of the $C_8H_7F-Ar_2$ (1/1) Ionic Cluster Shown in Figure 1[a]

label	ν	$\delta\nu$	σ_{abs}	assignment
				$\tilde{B}^2A'' \leftarrow \tilde{X}^2A''$
1	17217	0	0.25	0_0^0
2	17611	394	0.09	28_0^1
3	18013	796	0.025	$28_0^2 + 23_0^1$
4	18365	1148	0.025	$19_0^1 + 23_0^1 28_0^1$
5	18660	1443	0.015	12_0^1
6	18827	1610	0.015	$23_0^2 + 9_0^1$
7	19074	1857	0.008	$12_0^1 28_0^1$
8	19252	2035	0.008	$23_0^2 28_0^1 + 9_0^1 28_0^1$

[a] The positions are given in cm^{-1} and σ_{abs} in 10^{-16} cm^2. The cross section values are those measured at the top of the bands in the experimental spectrum. The uncertainty is ±10 cm^{-1} for the positions and 30% of the values for the cross sections.

The photodissociation spectrum of 4FSTY$^+-$argon$_2$ (1/1) is composed of a vibronic system with its origin at 17 217 ± 10 cm^{-1}. That of 4FSTY$^+-$argon (1/0) is very similar, except for a frequency shift to the blue of 12 ± 10 cm^{-1} due to the van der Waals interaction: its observed origin is located at 17 229 ± 10 cm^{-1}. This position lies close to the position of the $\tilde{B}$ state measured by photoelectron spectroscopy at 1.99 eV.[42] Therefore, the observed vibronic system is assigned to the $\tilde{B}^2A'' \leftarrow \tilde{X}^2A''$ electronic transition. In addition, the vibronic system resembles that of the styrene$^+$ cation measured in an argon matrix.[43] Their origins are separated by about 800 cm^{-1}, which is very close when considering that the usual effect of the argon matrix is a large red shift. This indicates that the fluorine substitution weakly affects the position of this electronic excited state, as found from PES studies on fluorostyrene compounds where the second electronic states were inferred to involve orbitals from the vinyl group and ring chromophore but not those of the fluorine atom.[42] Indeed, the measured $\tilde{B} \leftarrow \tilde{X}$ electronic transition in fluorobenzene$^+$ has its origin at 21 075 cm^{-1},[18] which is much higher in energy. The oscillator strength of the presently measured electronic transition is found to be 0.014, which compares well with that calculated for the homologous transition in styrene$^+$, where $f = 0.06$.[44]

The frequencies of the band centroids for 4FSTY$^+-$argon$_2$ obtained from the Lorentzian fit, together with their absorption cross sections and tentative assignments, are listed in Table 1.

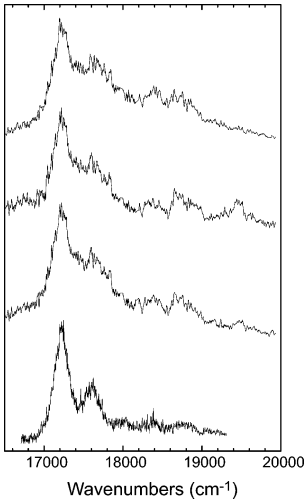

Figure 2. Photodissociation spectra of the 4-fluorostyrene cation measured through the main dissociation channels as well as that of the ionic complex for comparison. From top to bottom: H loss, F loss, C_2H_n loss. The vibronic bands appear much broader than those of the photodissociation spectrum of the weakly bound complex. It should be noted that special care was taken to minimize the laser intensity for the photodissociation step. The three spectra were slightly smoothed for clarity.

The Mulliken nomenclature is used.[40] The assignment relies on the calculated totally symmetric modes, those observed in the neutral ground and excited states and the ionic ground state, and are guided by the strong similarity with the styrene cation spectrum.[43] Two modes are found to dominate, their frequencies being 394 and 1148 cm^{-1}. They are assigned to modes ν_{28} and ν_{19}, respectively, according to harmonic frequency calculations[45] and ionic ground-state measurements.[39] Although mode ν_{28} is clearly observed in combination with others, the other assignments are only given tentatively because the fwhm smoothes out the vibronic structure and indeed many other modes could contribute. The most active mode, ν_{28}, involves mainly the symmetric deformation of the vinyl group, which is consistent with the nature of the electronic excitation.

The resonantly enhanced multiphoton dissociation spectrum of the bare cation could be measured by slightly increasing the photodissociation laser intensity. The main fragmentation channels were found to be the loss of one hydrogen atom, the loss of the fluorine atom, and the loss of a C_2H_n group presumably dominated by the C_2H_2 fragment.[46] Previous photodissociation spectroscopy studies of the styrene cation[46] and the fluorobenzene cation[2,47] indicate that a two-photon process should open these fragmentation channels. The electronic spectra are shown in Figure 2 together with that of $4FSTY^+-argon_2$ for comparison. These compare well, and the measured origin lies at 17 220 $\pm$ 25 cm^{-1}, which is consistent with the measured origins for the ionic complexes. However, it can be seen that the profile and intensity ratios differ, even considering the low signal-to-noise due to the difficulty of recording such broad spectra. In fact, saturation effects could not be avoided although the photodissociation laser intensity was minimized. Therefore the measured vibronic bands appeared much broader (fwhm up to 300 $\pm$ 30 cm^{-1}) with the vibrationally excited bands appearing stronger. Although the main aspect of the vibronic system is preserved, no identification of the individual vibronic bands was attempted due to the width and the low signal-to-noise ratio. These last spectra show that the REMPDS method is not well suited for electronic spectra composed of broad vibronic bands. On the contrary, the use of the argon atom tagging improves the results and accuracy very noticeably.

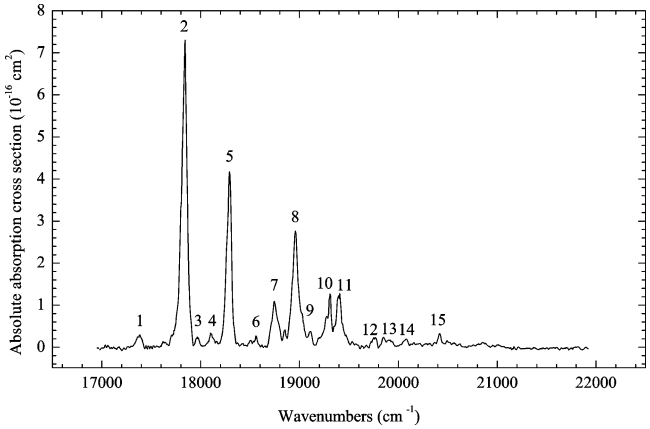

Figure 3. Photodissociation spectra of the $C_8H_6^+-Ar$ ionic complex. The labels of the bands are those used in Table 2. The laser photodissociation fluence was adjusted to allow observation of the weakest bands with a reasonable signal-to-noise ratio. The preparation of the complex was done using a resonant one-color two-photon scheme to show up the hot bands.

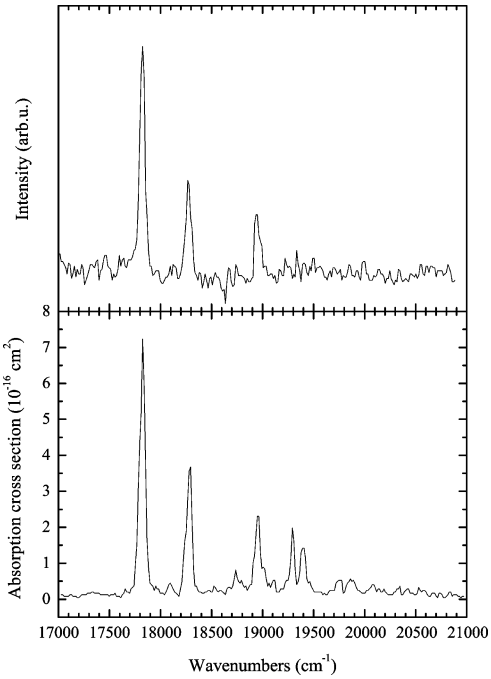

Figure 4. Photodissociation spectra of the $C_8H_6^+-Ar$ ionic complex taken in various conditions. Top panel: a two-color scheme through the $35_1(S_1)$ intermediate state was used to initially prepare the cation in its 35_1 vibrationally excited state in the electronic ground state (see text). Bottom panel: the cation was prepared in the vibrationless level of the electronic ground state and the photodissociation laser fluence was set to avoid any saturation effects. Note in this latter spectrum the slight difference in intensity ratio with that shown in Figure 3.

B. Phenylacetylene Cation. The photodissociation spectrum of the phenylacetylene$^+-$argon (1/0) ionic complex is shown in Figure 3. The cation was prepared by a R2PI scheme. The spectrum was already shown in a preliminary report,[11,48] but at that time a complete vibrational analysis was missing and the absorption cross section was not yet measured. The assignment is now straightforward because the PIRI spectrum with complete vibrational analysis of the bare cation was published recently.[35] Actually, some efforts have been put toward unraveling the fine structure of the vibronic bands that are not seen in the PIRI spectrum. The R2P2CI spectrum shown in Figure 4 reveals that band 1 is a hot band. The transition is assigned to the $\tilde{C}^2B_1 \leftarrow \tilde{X}^2B_1$ electronic transition origin at 17 835 $\pm$ 5 cm^{-1}.

TABLE 2: Band Center Positions (Absolute ν and Relative $\delta\nu$) and Absolute Absorption Cross Section (σ_{abs}) Obtained from the Photodissociation Spectrum of the $C_8H_6^+-Ar$ (1/0) Cluster Shown in Figure 3[a]

label	ν	$\delta\nu$	σ_{abs}	assignment
				$\tilde{B}^2B_1 \leftarrow \tilde{X}^2B_1$
1	17370	−465		13_1^0
2	17835	0	7.30	0_0^0
3	18100	265	0.31	24_0^2
4	18287	452	4.17	13_0^1
5	18557	722	0.27	$13_0^124_0^2$
6	18738	903	1.08	13_0^2
7	18953	1118	2.76	9_0^1
8	19302	1467	1.26	7_0^1
9	19396	1561	1.22	6_0^1
10	19755	1920	0.23	$7_0^113_0^1$
11	19842	2007	0.22	$9_0^113_0^2 + 6_0^113_0^1$
12	19910	2075	0.17	−
13	20076	2241	0.19	9_0^2
14	20412	2577	0.32	$9_0^1\,7_0^1$?

[a] The positions are given in cm^{-1} and σ_{abs} in 10^{-16} cm^2. The cross section values are those measured at the top of the bands in the experimental spectrum. The uncertainty is ± 5 cm^{-1} for the positions and 30% of the values for the cross sections. It should be noted that band 1 disappeared in the R2C2PI procedure, clearly indicating that it is a hot band (see Figure 4).

This assignment is based on comparison with previous PES data.[42,49] The van der Waals electronic shift measured by comparing the spectra of the complexes containing one and two argon atoms is found to be 10 ± 10 cm^{-1}, i.e., a small blue shift between the transitions. The origin value of the bare cation measured by PIRI was reported at 17 834 cm^{-1},[35] which is very close to the phenylacetylene$^+$−argon complex. In addition, the spectrum taken in a R2P2CI scheme that prepares the cation in its 35_1 state is shown in Figure 4 and appears to resemble that from the vibrational ground state. The oscillator strength deduced from the measured absorption cross section is found to be 0.16.

All the characteristics of the bands, together with their assignment, are reported in Table 2. Our spectrum confirms that modes ν_{13}, ν_9, ν_7, and ν_6 are the most active. Mode ν_{13} is observed to form a small progression, as observed in the $\tilde{A}^2A_2 \leftarrow \tilde{X}^2B_1$ transition in aniline$^+$,[26] where the vibrational progression was much longer, fluorobenzene$^+$,[2,18,47] and other substituted benzene cations.[7,50] The vibronic structure is very similar to that of the PIRI spectrum, except for the intensity ratios and band profiles. In our spectrum presented in Figure 3, the laser fluence was adjusted to permit a clear detection of the weakest bands. Although the intensities of these bands may be slightly overestimated, the observed intensity ratios appeared close to the intrinsic ones (see Figure 4). In the PIRI spectrum it is rather clear that strong saturation is observed, as stated by the authors.[35] The REMPD spectrum was also recorded (not shown here). The main fragment channels were the H loss and C_2H loss. As in 4-fluorostyrene$^+$, the spectrum is clearly broader and the "necessary" saturation smoothes out the fine profile of the bands.

IV. Discussion

A. Band Profiles Analysis. ***1. 4-Fluorostyrene$^+$.*** In the cases of 4FSTY$^+$−argon$_{1,2}$ the fwhm's used in the Lorentzian fit were very large and differed with the number of argon atoms. A study of the effect of the laser fluence revealed that no power saturation could explain these profiles because no variation could be observed. Therefore, two sources have to be considered: intramolecular dynamics and hot and/or sequence bands involving both intramolecular and intermolecular modes. It is well-known that aromatic cations are generally nonfluorescent[51] because of an efficient internal conversion (IC), which leads to lifetime broadening. An upper limit for this nonadiabatic process can be given by the shortest period of vibration,[24] i.e., ∼10 fs for a CH stretch leading to a fwhm of hundreds of cm^{-1}. Thus the broadness could be explained by lifetime broadening, but the contribution of a vibrational substructure has to be analyzed.

During the R2PI process an excess energy above the IP of 392 cm^{-1} for the bare molecule, 419 cm^{-1} for 4FSTY−argon (1/0), and up to 447 cm^{-1} for the chromophore bound to two argon atoms in the (1/1) conformation[32] may allow low-frequency vibrational modes of the ground state to be excited. Threshold PES (TPES) on styrene−argon clusters does not reveal a strong population in the intermolecular modes.[28] We expect that it should be the case for 4FSTY$^+$−argon$_{1,2}$ as well. Concerning the intramolecular modes, TPES studies on styrene[28] and MATI[39] on 4-fluorostyrene can be used. Unfortunatly that region of excess energy above the adiabatic IP was not reported in the MATI spectra of 4FSTY via the 0_0^0 (S_1) excitation. However, this information could be obtained using the MATI spectrum measured via the 23^1 excited state in the S_1 electronic state of neutral 4FSTY because a strong population of the vibrationless level of the cation is observed.[39] The spectra clearly indicate that the 28_1 state (at 390 cm^{-1} in 4FSTY$^+$) is populated, and the population of the 27_1 level at 425 cm^{-1} and 41_4 at 448 cm^{-1} are even more efficient.[39]

In the 4FSTY$^+$−argon$_n$ complexes a different population distribution of the intramolecular modes is expected, because the excess energies are different: 419 cm^{-1} for $n = 1$ and 447 cm^{-1} for $n = 2$. The states 27_1 at 425 cm^{-1} and 41_4 at 448 cm^{-1} appear to be accessible only for $n = 2$. No vibrational predissociation can take place because the binding energy is equal to about 550 cm^{-1} in the ionic ground state.[30,32] The cations that are produced in vibrationally excited states presumably undergo intra and intermolecular vibrational energy redistribution (IVR). Considering the difference in vibrational excitation, this process should be more efficient in 4FSTY$^+$−argon$_2$ and thus could lead to the observed band broadening. Although a R2P2CI scheme should clarify the situation, we consider the profile of the origin band recorded for 4FSTY$^+$−argon as a good indication of the intrinsic one for the $\tilde{B} \leftarrow \tilde{X}$ electronic transition because the excess energy above the ionization threshold seems small enough in this case to prevent extensive population of vibrationally excited states following ionization. It implies that the electronic relaxation of the $\tilde{B}$ state is dominated by an ultrafast internal conversion (IC), in the so-called statistical limit[52] according to the Lorentzian fit, and that the lifetime is therefore as low as 30 ± 5 fs.

2. Phenylacetylene$^+$. In Figure 5, a series of "close-ups" of some bands in the photodissociation spectra of phenylacetylene$^+$−argon$_{1,2}$ are shown. They involved different ionization schemes to prepare the cations. As a preliminary remark the TPES study of Dyke et al.[28] did not reveal a strong change in geometry upon ionization for the argon atom located on the ring binding site. Therefore it seems plausible that no intermolecular modes are populated during the ionization process.

The origin band of the phenylacetylene$^+$−argon prepared in its vibrational ground state shows substructure (panel a of Figure 5). It is composed of "individual" peaks having a fwhm of ≈8 cm^{-1} and separated by about 16 cm^{-1}, the spacing decreasing slightly with increasing position. It is not seen if the cation is prepared in a one-color scheme (not shown here), i.e., with an

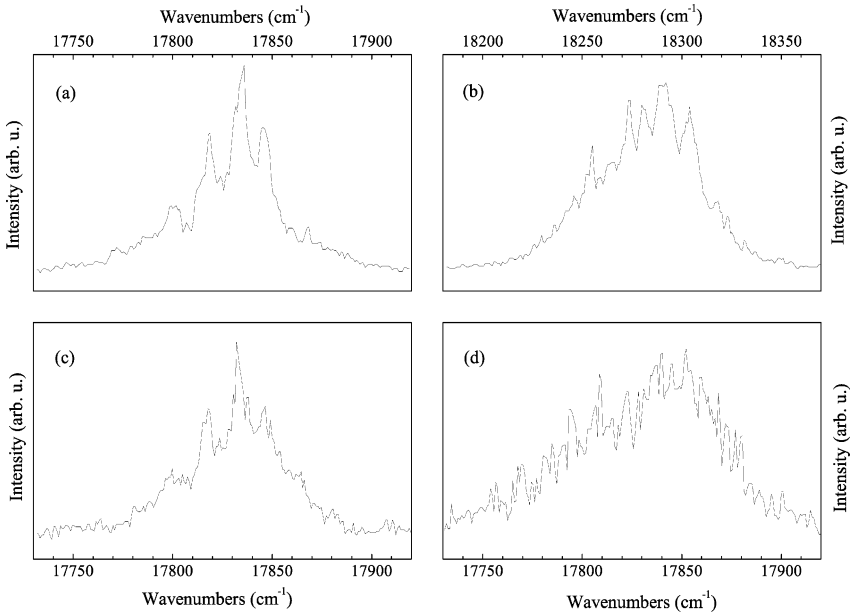

Figure 5. Close-ups of various bands of the $\tilde{C} \leftarrow \tilde{X}$ photodissociation spectra of the $C_8H_6^+-Ar_{1,2}$ ionic complexes taken in various conditions. (a) Origin of the electronic transition measured in the $C_8H_6^+-Ar$ cation prepared via a two-color scheme via the $0(S_1)$ intermediate state, i.e., prepared in the vibrationless level of the electronic ground state. (b) Band 13_0^1 in the same conditions as (a). (c) Region of the origin of the electronic transition measured with the cation prepared in its 35_1 vibrationally excited state in the electronic ground state. (d) Origin band of the $C_8H_6^+-Ar_2$ prepared in a one-color scheme.

excess energy of 706 cm^{-1} above the ionization potential. This excess is deduced from our own measurement of the ionization potential, 8.821 eV, because the published values differ slightly: 8.825 eV[28] and 8.195 eV.[39] However, the van der Waals IP shift due to one argon is found to be the same as in ref 28. Panel b of Figure 5 shows the profile of the 13_0^1 vibronic band under identical preparation. A substructure is also seen, but the profile is clearly different from that of the origin band. Therefore it cannot be explained by a vibrational population in the ionic ground state, as was proposed earlier.[48] This difference points toward intrinsic profiles. Such line shapes are presumably the result of an electronic relaxation dominated by a $\tilde{C} \rightarrow \tilde{B}$ IC in the intermediate case, as in well-known cases like pyrene,[53] ovalene,[54] and others (see ref 24). PES data enabled the location of the $\tilde{B}$ state, which is only 0.67 eV below the presently investigated $\tilde{C}$ state. Although no major geometry changes are found between the $\tilde{X}^2B_1$ ground and the $\tilde{C}^2B_1$ excited electronic states,[35] it is expected that change occurs on the substituent in the $\tilde{B}^2B_2$ state as found for the S_2 electronic state of its neutral PA, where a conical intersection with the S_1 state is found.[55] Interestingly, in the investigation of the electronic relaxation of neutral benzene derivatives by time-resolved PES, lifetimes as short as ~50 fs were measured for styrene and phenylacetylene.[25] However, in the latter case the only report of the $S_2 \leftarrow S_0$ electronic transition[56] reveals a broad profile (fwhm $\geq$ 250 cm^{-1}) without evidence of substructure although the energy gap, 0.75 eV, which is comparable to that found in the cation.

Panel c in Figure 5 shows the profile observed in the $\tilde{C} \leftarrow \tilde{X}$ origin region under 35_1 ($\tilde{X}$) (at 504 cm^{-1} [28]) scheme preparation. This profile is remarkably similar in shape and position yet less structured to that in panel a, although the frequency of mode ν_{35} is expected to increase by $\approx$5 cm^{-1} upon $\tilde{X} \rightarrow \tilde{C}$ electronic excitation.[35] It is consistent with the measured spectrum shown in Figure 4, which again closely resembles that obtained from the vibrationless ground state. It seems to show that we do not observe the expected pure 35_1^1 band. It may be understood if intra- and intermolecular vibrational energy transfer take place. The resulting state should therefore not have a peculiar mode coupling, as seen through the line shape of the 13_0^1 band when compared to that of the 0_0^0 band. Only a noticeable smoothing should be observed. Panel d in Figure 5 shows the profile of the origin band of the PA^+-Ar_2 complex prepared in a R2PI scheme. That of the complex with one argon atom is similar apart from the vdW electronic shift. In these cases the profiles are smoothed and no substructures may be seen.

B. Intramolecular Dynamics in the Benzene Derivatives. The benzene derivatives were the class of molecules that revealed that nonradiative processes, and in particular the IC in cations, dominated the relaxation of electronically excited states. It was shown that indeed most of the aromatic cations were not fluorescent.[51] For those that do exhibit a measurable emission spectrum, the fluorescence quantum yields were measured, enabling tendencies in the evolution of the radiationless transition rates to be deduced.[27,51] However, extension to short lifetimes was not possible in the early 1980s but due to recent advances by some research groups it now appears possible. For the nonfluorescent cations, the excited-state lifetimes can be drawn from the fwhm's of the origin bands of electronic transitions when available, and a contribution of the rotational profile is taken into account when necessary.[57] This is included in the reported uncertainty limits of the nonradiative rates. All the data found in the literature completed by our present measurements are listed in Table 3.

A plot of the nonradiative rate, k_{IC}, against the energy gap ΔE between the prepared electronic excited state and that immediately below is given in Figure 6. It appears that the general trend is consistent with the energy gap law,[58] except for fluorobenzene$^+$ (number 7), phenol$^+$ (number 10), and benzene$^+$ (number 12). It can be seen in Figure 6 that the rates extend over 7 orders of magnitude. For the "slow" regime, the smallest rates are limited by fluorescence quantum yields close to unity; i.e., only upper limits are given. For the "ultrafast" regime, illustrated by the case of 4FSTY$^+$, the rates reach the physical limitation of 10^{14} s^{-1} of the IC mentioned above

TABLE 3: Rate of Internal Conversion for Some Ionic Benzene Derivatives[a]

	molecular ion	ΔE (eV)	k_{IC} (s^{-1})	ref
1	1,3,5 $C_6H_3F_3$	2.71	$\approx 10^6$	22
2	C_6F_6	2.68	$\approx 10^6$	22
3	1,2,3 $C_6H_3F_3$	2.65	$5.42 \pm 0.18\ 10^6$	22
4	1,2,3,4 $C_6H_2F_4$	2.57	$2 \pm 1.01\ 10^6$	22
5	C_6HF_5	2.54	$\approx 10^6$	22
6	1,2,3,5 $C_6H_2F_4$	2.52	$\approx 10^6$	22
7	C_6H_5F	2.43	$1 \pm 0.3\ 10^{12}$	2
8	1,2,4,5 $C_6H_2F_4$	2.35	$1.22 \pm 0.18\ 10^7$	22
9	1,3 $C_6H_4F_2$	2.31	$\approx 10^9$	22
10	C_6H_5OH	2.2	$8 \pm 6\ 10^{11}$	4
11	1,2,4 $C_6H_3F_3$	2.19	$8.6 \pm 1.72\ 10^7$	22
12	C_6H_6	2.18	$2 \pm 1\ 10^{12}$	2
13	1,3 $C_6H_4Cl_2$	1.86	$3 \pm 2\ 10^{11}$	21
14	C_6H_5Cl	1.63	$8 \pm 6\ 10^{11}$	16
15	1,4 $C_6H_4Cl_2$	1.49	$1 \pm 0.5\ 10^{12}$	6
16	$C_6H_5NH_2$	1.31	$8 \pm 2\ 10^{12}$	26
17	1,3 $C_6H_4Br_2$	1.2	$5 \pm 4\ 10^{11}$	51
18	1,4 $C_6H_5Br_2$	1.2	$5 \pm 4\ 10^{11}$	51
19	4-$C_6H_4FC_2H_3$	1.01	$3.4 \pm 0.4\ 10^{13}$	this work

[a] Data are taken from the literature and are either deduced from the fluorescence quantum yield or derived from the experimental line width of the origin band when the cation is not fluorescent (see text). The energy gap ΔE is that between the observed excited state and the electronic state immediately below. Except for the aniline cation where it is the $\tilde{A}$ state, all the observed states are the $\tilde{B}$ states. The energy gap values are taken from photoelectron spectra, and the values are referenced in the cited paper for the rate.

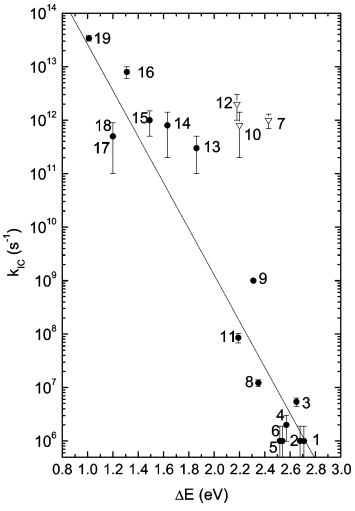

Figure 6. Plot of the nonradiative rate k_{IC} of the vibrationless level of the excited states versus the energy gap ΔE. The circles are associated with the cations where the electronic excited states are "π" states; the open triangles, with the "σ" states (see text). The line is a linear fit (semilog scale) of the first group to outline the apparent energy gap law type tendency. It should be noted that the smallest values are those for states with fluorescence quantum yield close to unity and the largest are those close to the shortest period of nuclear vibrations.

(section IV.A). The straight line in this figure corresponds to a linear fit of $\ln(k_{IC})$ against ΔE.

Such a fit tends to outline a trend: the shorter the gap, the faster the electronic relaxation. This may be rationalized in the form of an exponential energy gap law. However, from this set of data, it is not clear whether the distribution implies that below a threshold of about 2.2−2.4 eV electronic excited-state lifetimes become very short because of the presence of a conical intersection. If analyzed within the frame of the standard radiationless transitions theory (see, for instance, refs 52 and 24), the dispersion of data from the exponential fit may find an explanation in the fact that most of the cations revealed some degree of geometry change between electronic states. This suggestion is reinforced by the fact that IVR assisted IC was inferred for some cations.[22,26,50] All of this suggests that a tendency may exist but a regular evolution along the 7 orders of magnitude is not to be expected.

As can be seen in Figure 6, when the exponential dependence is considered, fluorobenzene$^+$, benzene$^+$, and phenol$^+$ appear to be exceptions. In fact, the electronic excited states of these three cations are known to involve σ orbitals whereas in all the other compounds the electronic transitions correspond to $\pi \leftarrow \pi$ electron promotion.[50,51] It is due to the influence of the substituent on the ordering of the orbitals in the cations.[50] Their ultrafast dynamics are thus probably due to the strong geometry change accompanying the electronic excitation, which is expected to lead to a conical intersection.[59] It appears that the electronic structure of the benzene derivatives reveal specific orbital mixing between the aromatic ring and the substituent, which in turn leads to dispersed electronic relaxation rates along an energy gap law type trend.

Thus, the open question is that, although an energy gap law seems capable of explaining the ultrafast decay of the excited state as shown in Figure 6, would the IC in the statistical limit lead to such short lifetimes, or is it systematically mediated by a conical intersection? By analysis of the PES spectra of all cations listed in Table 3, most do not reveal such extended changes as in the three cations cited above, behavior that renders a conical intersection more difficult to speculate. Thus a final answer should come from additional experimental data on the electronic excited-state lifetimes for ionic benzene derivatives for which the energy gap is in the 2 eV range because the dynamics across conical intersections should not, a priori, reveal a dependence on the electronic energy gap. In addition, potential energy surfaces calculations such as that done on neutral PA[55] should help to locate the eventual conical intersections.

V. Conclusion

The electronic absorption spectra of two ionic benzene derivatives were measured by mass spectrometric monitoring of photodissociation. Different laser techniques have been used, enabling a comparison of them. It appears that multiphoton dissociation of the bare cation is applicable when only two photons are necessary to open fragmentation channels but tends to largely broaden the spectra, in particular if the vibronic bands are intrinsically broad. On the other hand, measurement of the resonant ejection of a weakly bound atom gives a direct access to the cold absorption spectrum, which is complementary to the PIRI technique that allows preparation of the cation in different vibrational states and opens the way to mode assignment in the spectrum.

The electronic spectra of these nonfluorescent cations gave the opportunity to analyze the evolution of IC in aromatic cations. These measurements complete the set of data available in the literature in the ultrafast regime as given by frequency resolved spectra. It seems that the rates tend to follow an energy gap law over more than 7 orders of magnitude. According to this, the phenylacetylene cation is inferred to exhibit an intermediate case behavior, showing that most of the situations can be met with aromatic cations. However, some data should be measured more precisely in the range of intermediate energy gaps to confirm the tendency and to allow the IC to be properly rationalized in terms of the energy gap law or to infer a dominant role of the conical intersection to explain ultrafast dynamics.

References and Notes

(1) Dimauro, L.; Heaven, M.; Miller, T. *Chem. Phys. Let.* **1984**, *104*, 526.
(2) Walter, K.; Boesl, U.; Schlag, E. *Chem. Phys. Let.* **1989**, *162*, 261.
(3) Tsuchiya, Y.; Fujii, M.; Ito, M. *J. Chem. Phys.* **1989**, *90*, 6965.
(4) LeClaire, J.; Anand, R.; Johnson, P. *J. Chem. Phys.* **1997**, *106*, 6785.
(5) Kim, B.; Weber, P. *J. Phys. Chem.* **1995**, *99*, 2583.
(6) Dzhonson, A.; Gerlich, D.; Bieske, E.; Maier, J. P. *J. Mol. Struct.* **2006**, *795*, 93.
(7) Duncan, M. A. *Int. J. Mass Spectrom.* **2000**, *200*, 545.
(8) Bieske, E. J.; Dopfer, O. *Chem. Rev.* **2000**, *114*, 120.
(9) Bieske, E. J. *Chem. Soc., Faraday Trans.* **1995**, *91*, 1.
(10) Pino, T.; Boudin, N.; Bréchignac, P. *J. Chem. Phys.* **1999**, *111*, 7337.
(11) Bréchignac, P.; Pino, T.; Boudin, N. *Spectrochim. Acta Part A* **2001**, *57*, 745.
(12) Boesl, U.; Weinkauf, R.; Walter, K.; Weickhardt, C.; Schlag, E. *J. Phys. Chem.* **1990**, *94*, 8567.
(13) Boesl, U.; Weinkauf, R.; Weickhardt, C.; Schlag, E. *Int. J. Mass Spectrom. Ion Processes* **1994**, *131*, 87.
(14) Boesl, U. *J. Phys. Chem.* **1991**, 95, 2949.
(15) Lemaire, J.; Dimicoli, I.; Botter, R. *Chem. Phys.* **1987**, *115*, 129.
(16) Ripoche, X.; Dimicoli, I.; Calvé, J. L.; Piuzzi, F.; Botter, R. *Chem. Phys.* **1988**, *124*, 305.
(17) Johnson, P.; Zhu, L. *Int. J. Mass Spectrom. Ion Processes* **1994**, *131*, 193.
(18) Anand, R.; LeClaire, J.; Johnson, P. *J. Phys. Chem.* **1999**, *103*, 2618.
(19) Taylor, D.; Goode, J.; LeClaire, J.; Johnson, P. *J. Chem. Phys.* **1995**, *103*, 6293.
(20) Kimura, K.; Katsumata, S.; Achiba, Y.; Yamazaski, T.; Iwata, S. *Handbook of He(I) Photoelectron Spectra of Fundamental Organic Molecules*; Japan Scientific Press: Tokyo, 1981; see also references therein.
(21) Maier, J. P.; Marthaler, O. *Chem. Phys.* **1978**, *32*, 419.
(22) Maier, J. P.; Thommen, F. *Chem. Phys.* **1981**, *57*, 319.
(23) Yu, L.; Forster, S.; Williamson, J.; Miller, T. *J. Chem. Phys.* **1990**, *92*, 5794.
(24) Medvedev, E.; Osherov, V. *Radiationless Transitions in Polyatomic Molecules*; Chemical Physics Vol. 57; Springer-Verlag: Berlin, 1995.
(25) Lee, S.-H.; Tang, K.-C.; Chen, I.-C.; Schmitt, M.; Shaffer, J.; Schultz, T.; Underwood, J.; Zgierski, M.; Stolow, A. *J. Phys. Chem. A* **2002**, *106*, 8979.
(26) Pino, T.; Boudin, N.; Douin, S.; Bréchignac, P. *Chem. Phys. Lett.* **2006**, *419*, 356.
(27) Leach, S.; Dujardin, G.; Taieb, G. *J. Chim. Phys.* **1980**, *77*, 705.
(28) Dyke, J.; Ozeki, H.; Takahashi, M.; Cockett, M.; Kimura, K. *J. Chem. Phys.* **1992**, *97*, 8926.
(29) Consalvo, D.; van der Avoid, A.; Piccirillo, S.; Coreno, M.; Giardini-Guidoni, A.; Mele, A.; Snels, M. *J. Chem. Phys.* **1993**, *99*, 8398.
(30) Piccirillo, S.; Consalvo, D.; Coreno, M.; Giardini-Guidoni, A.; Douin, S.; Parneix, P.; Bréchignac, P. *Chem. Phys.* **1994**, *187*, 97.
(31) Coreno, M.; Piccirillo, S.; Giardini-Guidoni, A.; Mele, A.; Palleschi, A.; Bréchignac, P.; Parneix, P. *Chem. Phys. Lett.* **1995**, *236*, 580.
(32) Douin, S.; Picirillo, S.; Bréchignac, P. *Chem. Phys. Lett.* **1997**, *273*, 389.
(33) Lakin, N.; Pietraperzia, G.; Becucci, M.; Castellucci, E.; Coreno, Giardini-Guidoni, M. A.; van der Avoid, A. *J. Chem. Phys.* **1998**, *108*, 1836.
(34) Siglow, K.; Neusser, H. J. *Chem. Phys. Lett.* **2001**, *343*, 475.
(35) Xu, H.; Johnson, P. M.; Sears, T. J. *J. Phys. Chem. A* **2006**, *110*, 7822.
(36) Douin, S.; Parneix, P.; Amar, F.; Bréchignac, P. *J. Phys. Chem. A* **1997**, *101*, 122.
(37) Pino, T.; Parneix, P.; Douin, S.; Bréchignac, P. *J. Phys. Chem. A* **2004**, *108*, 7364.
(38) Kwon, C.; Kim, H.; Kim, M. *J. Phys. Chem. A* **2003**, *107*, 10969.
(39) Georgiev, S.; Neusser, H. *J. Chem. Phys*. **2004**, *120*, 8015.
(40) Hollas, J.; Hussein, M. B. *J. Mol. Spetrosc.* **1991**, *145*, 89.
(41) Hermine, P.; Parneix, P.; Coutant, B.; Amar, F.; Bréchignac, P. *Z. Phys. D* **1992**, *22*, 529.
(42) Ajo, D.; Tondello, E.; Marcuzzi, F.; Modena, G. *J. Cryst. Spec. Res.* **1989**, *19*, 683.
(43) Andrews, L.; Harvey, J.; Kelsall, B.; Duffey, D. *J. Am. Chem. Soc.* **1981**, *103*, 6415.
(44) Kesper, K.; Münzel, N.; Pietzuch, W.; Specht, H.; Schweig, A. *J. Mol. Struct.* **1989**, *200*, 375.
(45) Granadino-Roldán, J.; Fernández-Gómez, M.; Navarro, A.; Jayasooriya, U. *Phys. Chem. Chem. Phys.* **2003**, *5*, 1760.
(46) Fu, E. W.; Dunbar, R. C. *J. Am. Chem. Soc.* **1978**, *100*, 2283.
(47) Bieske, E.; Rainbird, M.; Knight, A. *J. Phys. Chem.* **1990**, *94*, 3962.
(48) Boudin, N.; Pino, T.; Bréchignac, P. *J. Mol. Struct.* **2001**, *563*, 209.
(49) Lichtenberger, D.; Renshaw, S.; Bullock, R. *J. Am. Chem. Soc.* **1993**, *115*, 3276.
(50) Johnson, P.; Anand, R.; Hofstein, J.; LeClaire, J. *J. Electron. Spectrosc. Relat. Phenom.* **2000**, *108*, 177.
(51) Maier, J. P.; Marthaler, O.; Mohraz, M. *J. Chim. Phys.* **1980**, *77*, 661.
(52) Avouris, P.; Gelbart, W.; El-Sayed, M. *Chem. Rev.* **1977**, *77*, 793.
(53) Mangle, E.; Topp, M. *J. Phys. Chem.* **1986**, *90*, 802.
(54) Amirav, A.; Even, U.; Jortner, J. *J. Phys. Chem.* **1981**, *85*, 309.
(55) Amatatsu, Y. *J. Phys. Chem. A* **2006**, *110*, 4479.
(56) Leopold, D.; Hemley, R.; Vaida, V.; Roebber, J. *J. Chem. Phys.* **1981**, *75*, 4758.
(57) Amirav, A.; Jortner, J. *Chem. Phys.* **1984**, *85*, 19.
(58) Englman, R.; Jortner, J. *Mol. Phys.* **1970**, *18*, 145.
(59) Yarkony, D. R. *J. Phys. Chem. A* **2001**, *105*, 6277.